RADIATION RESEARCH **156**, 210–214 (2001)
0033-7587/01 $5.00

The Columbia University Single-Ion Microbeam

Gerhard Randers-Pehrson,[1] Charles R. Geard, Gary Johnson, Carl D. Elliston and David J. Brenner

Center for Radiological Research, Radiological Research Accelerator Facility, Columbia University, Irvington, New York 10533

Randers-Pehrson, G., Geard, C. R., Johnson, G., Elliston, C. D. and Brenner, D. J. The Columbia University Single-Ion Microbeam. *Radiat. Res.* 156, 210–214 (2001).

A single-ion microbeam facility has been constructed at the Columbia University Radiological Research Accelerator Facility. The system was designed to deliver defined numbers of helium or hydrogen ions produced by a van de Graaff accelerator, covering a range of LET from 30 to 220 keV/μm, into an area smaller than the nuclei of human cells growing in culture on thin plastic films. The beam is collimated by a pair of laser-drilled apertures that form the beam-line exit. An integrated computer control program locates the cells and positions them for irradiation. We present details of the microbeam facility including descriptions of the collimators, hardware, control program, and the various protocols available. Various contributions to targeting and positioning precision are discussed along with our plans for future developments. Beam time for outside users is often available (see www.raraf.org).

INTRODUCTION

The use of microirradiation techniques in radiation biology dates back to the 1950s to the work of Zirkle and colleagues (*1*). There has been a recent resurgence of interest (*2–4*) in single-particle/single-cell microbeams, because we are now able to take advantage of new developments in particle delivery, focusing and detection, image processing and recognition, and computer control, coupled with the benefits of newer assays of individual cellular response.

The biological interest in the microbeam stems from the potential to define the ionizing energy absorbed by a cell, in terms of space, time and quantity:

1. The microbeam allows irradiation of many cells, each in a highly localized *spatial* region, such as part of the nucleus, or the cytoplasm, or through the immediate neighbor cells of a given cell. This capability allows questions regarding cell-to-cell communication, functionality of sub-components within the cell, and intracellular communication, to be addressed directly. Conversely, microbeam techniques allow selected cells or subcellular components in an irradiated population to remain *unirradiated*, allowing, for example, direct investigation of ''bystander'' effects. The microbeam also allows particles to be passed through a cell with a known *temporal* separation to investigate, for example, the dynamics of cellular repair.
2. At the low doses of relevance to environmental radiation exposure, individual cells only rarely experience traversals by densely ionizing particles, the intervals between the tracks typically being months or years. The biological effects of exactly one particle are unknown because, due to the random (Poisson) distribution of tracks, this cannot practically be simulated in the laboratory using conventional broad-field exposures. Microbeam techniques can overcome this limitation by delivering exactly one particle (or more) per cell nucleus or other subcellular target.

[1] Author to whom correspondence should be addressed at Center for Radiological Research, Radiological Research Accelerator Facility, Columbia University, 136 South Broadway, Irvington, NY 10533; e-mail: gr6@columbia.edu.

MATERIALS AND METHODS

A single-ion microbeam facility comprises a number of elements arranged to deliver counted numbers of ions to a chosen biological target reliably. The elements are: (1) a source of ions of the appropriate energy, (2) a means of limiting the location of the ions to an area less than the area of the target, (3) a means of locating and moving the biological targets to the beam position, (4) a means of detecting each ion as it traverses the target, and (5) a means of shutting off the beam after the arrival of the chosen number of ions. The characteristics of each of these elements determine the type of experiment that can be performed at the facility. An overall schematic of the facility is presented in Fig. 1.

Van de Graaff Accelerator

The source of ions for our microbeam is a model D1, 4.2 MV van de Graaff accelerator. This machine, which was originally the injector for the Cosmotron at Brookhaven National Laboratory, was converted to a dedicated radiobiology facility in 1966 and later moved to Irvington, NY, where it presently operates. The terminal is fitted with a duo-plasmatron ion source, which can produce beams of the isotopes of hydrogen and helium. Most of the work to date on the microbeam has been performed with α particles of 6 MeV corresponding to an LET of approximately 90 keV/μm at the center of the cells. Experiments can be performed with stopping α particles or with hydrogen ions with a lowest LET of 30 keV/μm, limited only by the transparency of the collimator system.

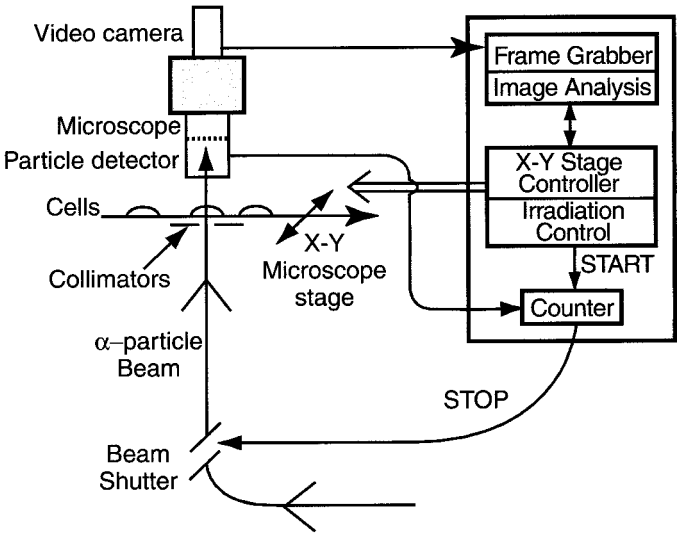

FIG. 1. Schematic drawing showing the overall layout of the microbeam facility and the integrated control system.

Collimator

The area of the beam of ions can be limited either by collimation or by focusing. For the present system, we chose to use collimation because of the simplicity of setup and operation compared to focused systems. There is a preliminary collimator with a 2-mm aperture, located 1.3 m before the final collimator system. The final collimator system (Lenox Laser, Phoenix, MD) consists of a pair of apertures laser-drilled in 12.5-μm-thick stainless steel foils and separated by a 300-μm spacer, as shown in Fig. 2. The limiting aperture is a 5-μm-diameter hole in the first foil. The second aperture, which is 6 μm in diameter, acts as an anti-scatter element. The relative alignment of the two apertures is fixed during manufacture. A scanning electron microscope was used to observe a series of holes drilled, in the same stainless steel material as the final collimator system, like the perforations of a postage stamp and then torn apart. As

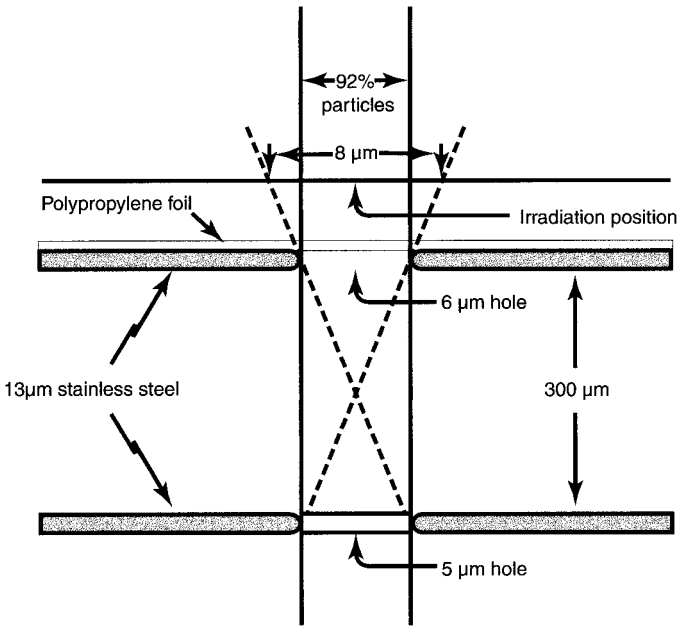

FIG. 2. Collimator geometry. Note that the horizontal dimensions have been expanded by a factor of 20.

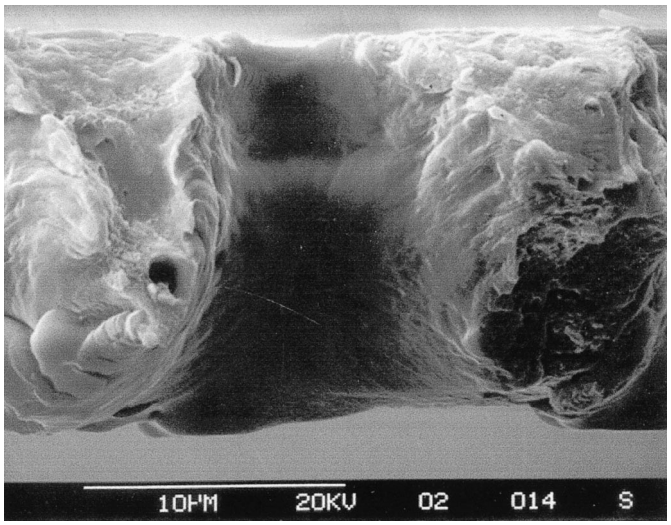

FIG. 3. Scanning electron micrograph of the collimator aperture.

seen in Fig. 3, the edges of the holes are approximately toroidal in shape with about a 12-μm radius.

In Fig. 4, we show the final collimator system, which is mounted in the shallow recess of a snout projecting from the end of the beam line. The center of the collimator system is located at the focus of a spherical gimbal mount. This allows alignment of the system with respect to the incoming beam without moving the exit aperture with respect to the center axis of the microscope objective. Two micrometers, positioned at right angles to each other, are used to align the final collimator system to the beam. The optimal position is found by iteratively tuning one micrometer at a time for a maximum percentage of full-energy particles measured in the detector. A typical iteration is shown in Fig. 5. Finally, a thin polypropylene sheet is stretched over the assembly to make a vacuum window.

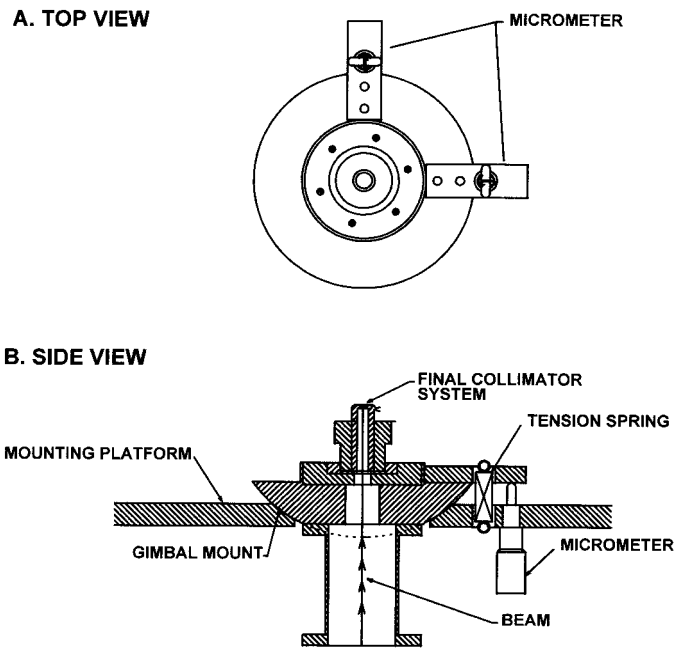

FIG. 4. Top (panel A) and side (panel B) views of the final collimator system, showing the spherical gimbal mount, adjusted using orthogonal micrometers. This setup is used to align the collimator system with the incoming beam.

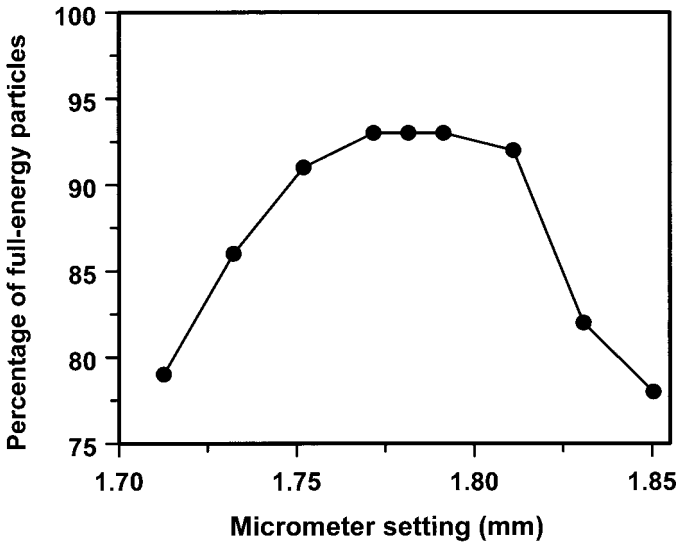

FIG. 5. Representative alignment scan for collimator apertures, showing the percentage of counts that appear in the full-energy peak as a function of the micrometer setting. The flat-topped region is consistent with the geometry shown in Fig. 2.

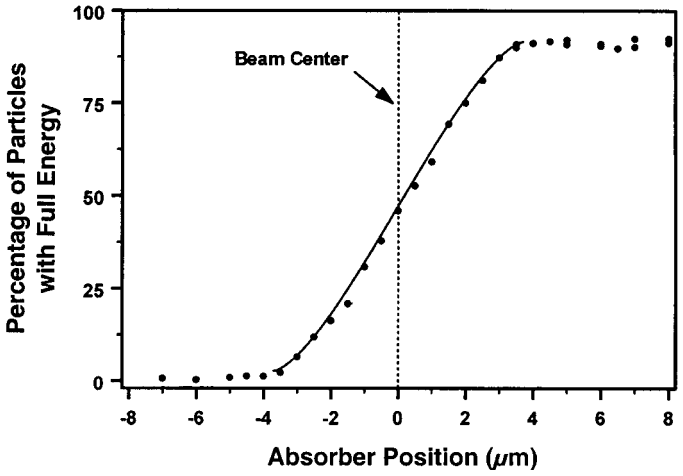

FIG. 6. Profile of the core of the beam. The percentage of the beam in the full-energy peak was measured by moving the edge of a Mylar absorber across the beam position. The curve represents the anticipated results of this experiment for a circular beam in which 92% of the particles are within a radius of 3.7 μm.

Monte Carlo modeling of this geometry and comparison to the energy spectrum of transmitted particles indicates that about 92% of them are within the nonscattered core of the beam, originally having a diameter of 5 μm, spreading to 7 μm due to Coulomb scattering in the exit window and air gap. Figure 6 shows a measurement of the core diameter. This profile was obtained by moving the edge of a 15-μm-thick piece of Mylar between the exit aperture and the detector. When the Mylar intercepts the beam, the particles are removed from the full-energy peak, but still have sufficient energy to be counted. The curve in the figure represents the anticipated results of this experiment for a circular beam in which 92% of the particles are within a radius of 3.7 μm. Approximately 7% of the beam is contained in a halo, resulting from particles that scatter in the edge of the first aperture and then pass through the anti-scatter aperture, around the core. This halo has a radius of about 8 μm at the cell irradiation position. The remaining 1–2% of the particles are scattered by both apertures and appear at greater distances from the target position. The beam characteristics are appropriate for the originally intended targets for the microbeam, namely the nuclei of mammalian cells in culture.

Imaging and Control Program

The most important factor in determining the throughput of a microprobe system for irradiating cells is the ability of the microscopic video analysis system to recognize the targets and move them into position. Cells are grown attached to a 3.88-μm-thick film of polypropylene treated with CelTak. Polypropylene was chosen because it is nonfluorescent. The stock cell suspension is diluted so that a chosen number of cells will be contained in a 2-μl drop of medium. The cells are stained by exposure to a 50 n*M* solution of the vital DNA stain Hoechst 33342 for 30 min prior to analysis. This low stain concentration necessitates the use of a channel-plate image-intensified CCD camera (GenSysII and CCD-72, Dage-MTI, Michigan City, IN) to obtain a high-contrast image. A narrowband epifluorescence cube (XF-06, Omega Optical, Brattleboro, VT) selects the 366-nm line from a mercury arc lamp for the observation. The output from the lamp is reduced (~3×) by a neutral density filter placed in the light path. The video signal is captured by a Matrox Genesis image processing board using the Matrox Imaging Library (Matrox Electronic Systems, Dorval, Canada).

An integrated program written in Visual Basic under the Windows NT operating system controls the video analysis system and microscope stage motion. A large number of tasks need to be accomplished to deliver single particles to a specific cellular target.

First, a relationship must be established between the pixel location of an object in the microscope camera and the number of *x*-*y* steps needed to move that object to the target location. To simplify the procedure, the camera is rotated to eliminate the angular offset between the two coordinate systems. Stepping motor-driven stages (Daedal, Inc., Harrison City, PA), which are designed to move 0.1 μm per step, are currently used to move an object a fixed distance within the microscope image and then measure the corresponding number of pixels traversed. With the 6× objective (magnification is actually about 6.3) on the microscope, we obtained a calibration factor of 26.5 steps per pixel; for the 40× objective, we obtained a calibration factor of 4.2 steps per pixel. The origin of the coordinate systems is defined by grabbing images of laser light that has been directed through the collimator system from below the last bending magnet. The calibration factors and origins are maintained in the computer and used for all movement and measurement calculations.

The steps and time involved in irradiation are shown in Table 1. For each culture dish, the approximate locations of the attached cells are

TABLE 1
Timing of the Various Steps in the Microbeam Irradiation Protocol

Protocol step	Time
1. Remove dish from incubator, aspirate medium, and mount on microbeam stage.	45 s
2. Using Matrox Genesis imaging, grap 10 overlapping images using 6× objective, subtract background, correct for illumination variation, locate cells, and record location of nearest 40× frame.	15 s
3. Change to 40× lens.	10 s
4. Visit each frame containing at least one cell, auto-focus microscope, grab image, subtract background, correct for illumination nonuniformity, locate cells, and irradiate each (~5 cells per image).	(3 s)
5. Repeat step 4,100 times.	300 s
Total time per 500 cells:	6 min
5a. Alternatively (for larger cell numbers), repeat step 4,134 times with 15 cells per image (4.5 s per frame)	600 s
Total time per 2000 cells:	11 min

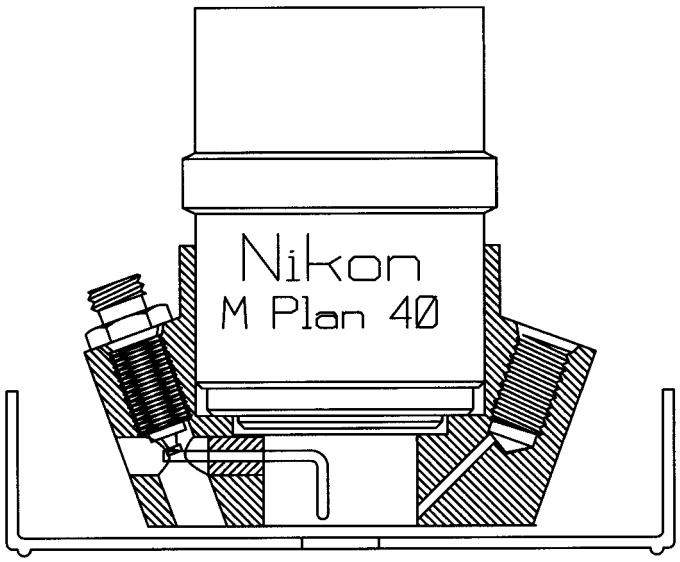

FIG. 7. Drawing of the pulsed ion counter mounted on the microscope objective. A small flow of P10 gas enters through the passage on the right. Another passage (not shown) brings humidified air + 5% CO_2 to the cells growing in the miniwell at the center of the culture dish.

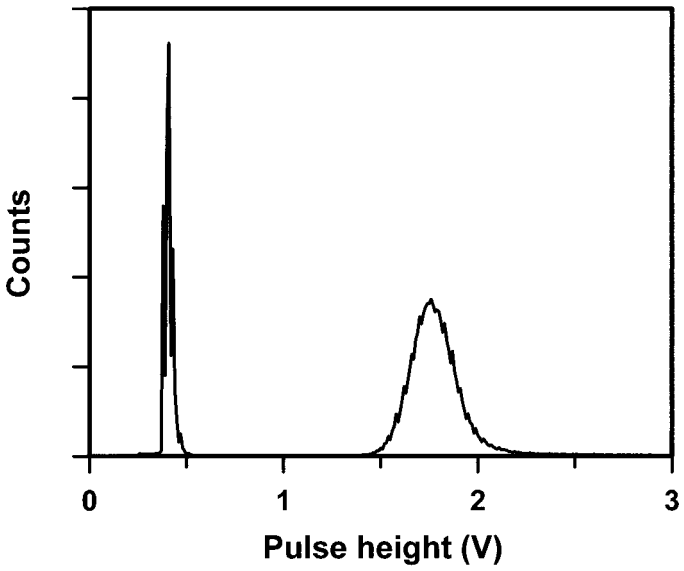

FIG. 8. Pulse-height spectrum from the ion counter. The threshold is normally set to 1.0 V, in the middle of the wide gap between signal and noise.

established using a low-magnification lens, so that time is not wasted imaging empty regions of the dish. This preliminary scan consists of 10 overlapping images arranged to cover the entire active area of the dish. Each image is a 10-frame average that has been smoothed and corrected for nonuniformity of illumination by a subroutine within the image analysis program. A threshold in intensity is set to separate the cells from the background. Upper and lower limits on the area of the objects are also used to discriminate against noncellular material in the dish. The locations determined are translated into defined fields of view for the high-magnification (40×) objective, which are then marked for imaging during the irradiation phase of the experiment.

In the final step of the experiment, each field of view that was found during the preliminary scan to contain at least one cell is moved into position, and a video image of the fluorescing nuclei is grabbed and analyzed. The centroid of each cell is calculated relative to the position of the exit aperture, this latter being defined by laser light shining through the collimator system as described previously. Each cell is sequentially positioned over the exit aperture by the stepping motors driving the microscope stage, and a chosen number of ions are delivered. Each nucleus within a given frame (~5–50) is visible on a monitor during the time of irradiation of that field (a few seconds). To test the accuracy of the stage drive system, a micrometer-scale grid was placed on the microscope stage. Several hundred or even a thousand moves were made away from reference points, given by fiduciary marks. Based on the accuracy of return to these fiduciary marks during testing, the combined precision of video analysis and stage positioning was estimated to be about 2 μm. The total time required to irradiate a single dish of 2,000 cells is approximately 11 min, corresponding to a throughput of around 11,000 cells/hour.

A list of locations that have been irradiated is maintained in the computer memory to prevent an accidental second irradiation. This is accomplished by assigning a single bit of computer memory to each 4 × 4-μm square within the dish. When a cell centroid is found, the corresponding bit is tested and, if the bit is off, the cell is irradiated. That bit and the eight surrounding ones are then turned on, preventing further targeting of that spot.

Ion Detection and Beam Shutter

To shut off the beam after delivering a certain number of ions, a reliable particle counter must be used. The primary counter, which is used when the ion beam has a sufficient residual range after passing through the target cells, is a pulsed ion counter filled with P10 gas (90% argon + 10% methane) and mounted on the high-power objective of the observation microscope, as shown in Fig. 7. Because the counter is above the cell culture, it is necessary to aspirate off all but a thin layer of medium for the duration of the radiation exposure. Humidified air with 5% CO_2 is passed through a passage in the counter body and over the culture to prevent dehydration. An entrance window of 2.5-μm-thick optically clear mica separates the gas in the counter from the gas over the cell culture. The path length for the particles is 8 mm.

When the counter is operated at 300 V, it has zero gas gain and thus provides a very stable signal, which is well separated from the noise, as shown in Fig. 8. The signal from the detector preamplifier is shaped by a standard amplifier, which feeds a single-channel analyzer, which in turn feeds a computer-controlled scaler. The gate period output of the scaler is fed to a high-voltage amplifier (Technisches Büro S. Fischer, Ober-Ramstadt, Germany) connected to electrostatic deflection plates to turn on the beam until the chosen number of particles has arrived. The rise and fall time of the deflection voltage is such that, approximately 4 times out of 10,000, there will be an extra particle delivered to the target. There is a background signal of about 7 counts per day due to α-particle activity in the glass elements of the microscope objective and in the body of the counter. The dark current with the electrostatic deflector off is less than one particle per hour.

A second detector is available for studies with particles stopping in the sample or with particles having a small residual range. It is a Schottky barrier detector constructed from a 2-μm-thick silicon wafer. It is placed in the beam path upstream of the cells, and provides a signal with excellent resolution and near 100% efficiency; the detector is, however, light-sensitive, which is generally inconvenient, and it is therefore used only for experiments where a detector downstream of the cells is inappropriate—specifically for particles stopping in the sample or for particles having a small residual range, and thus a high LET.

Alternative Irradiation Protocols

In addition to the standard protocol, in which we deliver a defined number of ions to the center of each cell nucleus present in the dish (*5*, *6*), we have developed and used several other irradiation protocols. The first of these new protocols was developed to irradiate the cytoplasm of each cell: The image analysis system defines the long axis of each cell,

after which the computer system delivered particles at two target positions, 8 μm away from each end of the cell. In these experiments, an exclusion zone around each fluorescent object (even if it is not identified as a nucleus) is automatically generated to ensure that the target positions from one nucleus are not accidentally within the nucleus of an adjacent cell. Wu *et al.* (*7*) have reported mutation induction by cytoplasmic irradiation using this technique.

We are using two variants of the standard protocol to study bystander effects. In the first variant [see, for example, Zhou *et al.* (*8*)], all of the cells are imaged, but the computer randomly irradiates only a chosen fraction of them. The second approach is to have a mixture of cells growing in the irradiation dish, but to have only a fraction of them stained with Hoechst and therefore visible to the image analysis system. The other cells might be stained with a dye of another color so they can be distinguished during later analysis. This is the technique used by Geard *et al.* (*9*).

Future Developments

It is clear from the present requests for beam time and discussion with users of the Columbia microbeam facility that two of the main directions for future use are to study bystander effects and to irradiate subcellular components. Both of these classes of experiments require better spatial resolution and the absence of a scatter-related beam halo. It is not possible to obtain a beam with those properties using a collimator system. We therefore designed and are currently building a new microbeam facility that will use a compound electrostatic lens system to obtain a beam spot of sub-micrometer precision (*10*). A prototype of the lens has been constructed and is undergoing tests on the present microbeam station. The prototype is expected to provide a beam with a diameter of 2 μm and essentially no scattered halo, while the final objective is to obtain a beam with a diameter of 0.3 μm, again with essentially no halo due to scattering.

Another limit of the present facility is that it can only be used to provide light ions (helium or hydrogen) with a limited range of LET. We plan to improve this range by installing a laser-driven ion source that will produce ions with masses up through iron, and thereby LETs up to 4,500 keV/μm. The combination of a large variety of ions and a focusing system will require new diagnostic techniques to ensure that all the parameters of the system are set to optimum values. We are currently designing an electron microscope to image the impact position of each ion by focusing the secondary electrons produced.

DISCUSSION

The Columbia University microbeam facility has proven capable of satisfying its original objective of studying the ability of single α particles to produce transformational and mutational events in mammalian cells irradiated through the nucleus. New studies involving subcellular targeting of cells and studies of bystander effects require upgrading the facility to obtain a smaller-diameter, halo-free beam. This work is currently in progress (*10*).

Beam time for outside users is often available, as described at www.raraf.org.

ACKNOWLEDGMENTS

The Columbia University Radiological Research Accelerator Facility (RARAF) is an NIH-Supported Resource Center. This work was supported by grant P41 RR-11623 from the National Center for Research Resources (NCRR) at the National Institutes of Health.

Received: January 31, 2000; accepted: May 14, 2001

REFERENCES

1. R. E. Zirkle and W. Bloom, Irradiation of parts of cells. *Science* **117**, 487–493 (1953).
2. C. R. Geard, D. J. Brenner, G. Randers-Pehrson and S. A. Marino, Single-particle irradiation of mammalian cells at the Radiological Research Accelerator Facility: Induction of chromosomal changes. *Nucl. Instrum. Methods* **B54**, 411–416 (1991).
3. J. M. Nelson, A. L. Brooks, N. F. Metting, M. A. Khan, R. L. Buschbom, A. Duncan, R. Miick and L. A. Braby, Clastogenic effects of defined numbers of 3.2 MeV alpha particles on individual CHO-K1 cells. *Radiat. Res.* **145**, 568–574 (1996).
4. M. Folkard, B. Vojnovic, K. M. Prise, A. G. Bowey, R. J. Locke, G. Schettino and B. D. Michael, A charged-particle microbeam: I. Development of an experimental system for targeting cells individually with counted particles. *Int. J. Radiat. Biol.* **72**, 375–385 (1997).
5. T. Hei, L-J. Wu, S-X. Liu, D. Vannais, C. A. Waldren and G. Randers-Pehrson, Mutagenic effects of a single and an exact number of α particles in mammalian cells. *Proc. Natl. Acad. Sci. USA* **94**, 3765–3770 (1997).
6. R. C. Miller, G. Randers-Pehrson, C. R. Geard, E. J. Hall and D. J. Brenner, The oncogenic potential of a single alpha particle. *Proc. Natl. Acad. Sci. USA* **96**, 19–22 (1999).
7. L-J. Wu, G. Randers-Pehrson, A. Xu, C. A. Waldren, C. R. Geard, Z-L. Yu and T. Hei, Targeted cytoplasmic irradiation with alpha particles induces mutations in mammalian cells. *Proc. Natl. Acad. Sci. USA* **96**, 4959–4964 (1999).
8. H. Zhou, G. Randers-Pehrson, C. A. Waldren, D. Vannais, E. J. Hall and T. Hei, Induction of a bystander mutagenic effect in mammalian cells. *Proc. Natl. Acad. Sci. USA* **97**, 2099–2104 (2000).
9. C. R. Geard, G. Randers-Pehrson, S. A. Marino, G. Jenkins-Baker, T. Hei, E. J. Hall and D. J. Brenner, Intra- and intercellular responses after cell-site-specific microbeam irradiation. *Radiat. Res.* **153**, 233 (2000). [extended abstract]
10. A. D. Dymnikov, D. J. Brenner, G. Johnson and G. Randers-Pehrson, Theoretical study of short electrostatic lens for the Columbia microbeam. *Rev. Sci. Instrum.* **71**, 1646–1650 (2000).